Journal of Hazardous Materials 189 (2011) 384–390

Contents lists available at ScienceDirect

Journal of Hazardous Materials

journal homepage: www.elsevier.com/locate/jhazmat

Facile synthesis of carbon supported copper nanoparticles from alginate precursor with controlled metal content and catalytic NO reduction properties

Sergios K. Papageorgiou*, Evangelos P. Favvas, Andreas A. Sapalidis, George E. Romanos, Fotios K. Katsaros

Institute of Physical Chemistry, N.C.S.R. DemokritosTerma Patriarchou Grigoriou & Neapoleos, 15310 Ag. Paraskevi Attikis, Athens, Greece

ARTICLE INFO

Article history:
Received 30 August 2010
Received in revised form
16 November 2010
Accepted 16 February 2011
Available online 23 February 2011

Keywords:
Alginate beads
Polyol
Nanoparticles
Carbon
Catalysis
NO reduction

ABSTRACT

A copper-nanoparticle-doped carbon was prepared from an alginate based precursor in a one step carbonisation–reduction procedure based on the modified polyol process. The ion exchange capacity of the precursor as well as the porosity, metal content, thermal properties, of the final product, were investigated. The preparation route leads to a porous carbon/copper composite with predefined metal loading reaching up to over 30% (w/w) of finely dispersed Cu nanoparticles of fairly uniform size. NO catalytic abatement evaluation showed high efficiency even at low temperatures compared to other recently reported carbon supported catalysts.

1. Introduction

Transition metal nanoparticles are found to have potential applications in various fields such as microelectronics [1], optical devices [2] catalysis [3], drug delivery [4], and hydrogen storage [5]. Since they exhibit remarkable physico-chemical properties which are not observed either in the individual molecules or in the bulk metals [6].

However unsupported metal nanoparticles are generally not easy to handle and form aggregates under drastic conditions found for example in catalytic applications such as reduction. In this respect they are usually fixed on supporting structures such as carbon [7,8].

Indeed carbon materials have been extensively used as nanoparticles supports in exhaust purification since even activated carbon itself can reduce NO_x to N_2 without addition of an external reducing agent [9–11]. The reaction between NO and carbonaceous materials normally occurs at temperatures above 500 °C [12] depending on the carbon chemical and porous properties [13,14]. However, a significant decrease of the temperature required for NO_x reduction [15,16] can be achieved when metal (alkali, alkaline-earth or some transition metals – Cr, Fe, Co, Ni and Cu) carbon supported catalysts are employed. In this case, NO_x dissociation results in the formation of oxygen that may deteriorate the carbon support at elevated temperatures and high NO_x concentration. Hence the development of a catalyst exhibiting significant dissociation activity at the lowest possible temperature (below 300 °C) is of paramount importance.

There are several ways to synthesize supported nanoparticles including impregnation [17], deposition–precipitation and co-precipitation [18], sonochemical reduction [19], chemical vapor impregnation [20], sol–gel [21] and microemulsion using organic stabilizing agents [17]. The control over either particle dimensions, including the particle size and distribution, or metal concentration in the composites remains the major drawback of these methods. For example, the traditional impregnation methods using liquid solutions as the processing medium cause not only particles agglomeration but also require a pre-treatment of the carbonaceous material in order to be able to adsorb metallic ions and a subsequent reduction step under hydrogen flow.

In the case of porous supports the commonly used approaches are based on sol–gel routes. For example, Baumann et al. [22] reported the synthesis of copper-doped carbon aerogels, utilizing a multi step process involving the sol–gel polymerization reaction of resorcinol followed by ion exchange and pyrolysis. Nevertheless, Cu nanoparticles of acceptable size (10–50 nm) were only formed in aerogels with low copper content (1–2%), while at

* Corresponding author. Tel.: +30 2106503636; fax: +30 2106511766.
E-mail address: spap@chem.demokritos.gr (S.K. Papageorgiou).

0304-3894/$ – see front matter © 2011 Elsevier B.V. All rights reserved.
doi:10.1016/j.jhazmat.2011.02.049

higher copper loadings (9–10% Cu) larger sizes were produced upon carbonisation.

An alternative way for the preparation of metal doped porous materials is based on the polyol process [23], a widely used method for the preparation of monodispersed metal nanoparticles involving a redox reaction of a metallic compound by a liquid polyol (e.g. ethylene glycol) serving both as solvent and reducing agent. In recent studies carbon supported copper nanoparticles [24] and SWCNTs supported palladium nanoparticles [25] were prepared with the polyol process but their synthesis involved a two step impregnation–reduction route with various limitations concerning the final products metal particle size, dispersion, and metal content.

Sodium alginate (SA) a natural linear copolymer of a-L-guluronic (G) and β-D-mannuronic (M) acid, contains many hydroxyl groups and has recently been used instead of ethylene glycol for the preparation of noble metal nanoparticles in solution according to the polyol process [26]. Taking advantage of its hydroxyl groups and its superior ion exchange capacity [27] one can incorporate metal ions into its polymeric matrix, which in the subsequent heating step under inert atmosphere during carbonisation, will be reduced to metallic particles. As the metal binding sites are distributed evenly all over the polymeric matrix, it is expected that the use of alginate-metal salts as a precursor for the preparation of carbon supported metal nanoparticles will provide materials with good dispersion in the final structure.

In this study we report a one step preparation route of carbon supported copper nanoparticles, based on a modified polyol process, involving the pyrolysis of copper loaded crosslinked alginate beads under inert atmosphere. The structural properties of the obtained material were characterised and its potential as a NO reduction catalyst was evaluated.

2. Experimental

2.1. Materials and methods

All reagents were of analytical grade and were used without further purification. Sodium alginate (SA) was extracted from *Laminaria digitata* biomass as described elsewhere [27]. For the crosslinking solution terephthalic aldehyde was purchased by SIGMA The metal solution for the alginate impregnation was prepared using $Cu(NO_3)_2{\cdot}3H_2O$.

Solutions of 4% (w/v) of SA were prepared by adding SA powder in ultrapure water under stirring for 12 h to ensure homogeneity. The SA solution was then outgassed for 24 h. The crosslinking solutions (acetalization) were prepared by mixing 2 g terephthalaldehyde, 2 ml HCl 5 N and 23 ml of methanol under stirring. The SA solution was added dropwise (Nisco Var J1) in the crosslinking solution with a ratio of 1:5. The resulting beads were left in the solution under stirring for 24 h to equilibrate and were subsequently filtered, washed with methanol and dried at room temperature.

The dried material was doped with copper by contacting the solid with metal solutions of different Cu^{2+} concentrations (10, 50, 100, 250 and 500 ppm at pH 4.5) for 24 h at 25 °C under stirring. The obtained beads were filtered, washed and dried in air at room temperature. The initial and final Cu^{2+} solution concentrations were determined by means of atomic absorption spectrometry. The dried alginate copper precursor was placed in a tubular furnace and carbonised at 800 °C under Ar, for 30 min, with a heating rate of 2 °C min^{-1}.

2.2. Characterisation techniques

The pore properties of the produced materials were determined by nitrogen adsorption–desorption isotherms at −196 °C using an automated volumetric system (AUTOSORB-1 – Krypton version – Quantachrome Instruments). Prior to their measurement, the samples were outgassed at 200 °C for 48 h.

The XRD patterns were recorded on a Rigaku R-AXIS IV Imaging Plate Detector mounted on a Rigaku RU-H3R Rotating Anode X-ray Generator.

Thermogravimetric analysis was performed on a SETARAM SETSYS Evolution 18 Analyser, in the range of RT–800 °C, with a heating rate 2 °C/min in a platinum crucible in order to monitor the carbonisation procedure, and a Jeol JSM 7401F Field Emission Scanning Electron Microscope equipped with Gentle Beam mode was employed to characterise the surface morphology of the C/Cu nanoparticles composites.

2.3. Catalytic experiments

The activity of the prepared material as a catalyst for NO reduction in the absence of oxygen was examined in a fixed bed reactor. The catalyst (300 mg) was packed in a quartz tube and the formed bed had a length of 8 cm and a volume of 0.5 cm^3. The applied gas mixture had a total flow rate of 36.5 ml/min giving rise to a gas hourly space velocity (GHSV) of 4500 h^{-1}.

The flow rate of each gaseous stream was controlled by means of electronic mass flow controllers (Bronkhorst F-200CV) of 2–100 ml min^{-1} full-scale for NO and 20–1000 ml min^{-1} for He. The feed composition was 5.2 vol.% NO, 0.16% N_2, 0.028% N_2O, N_2 and N_2O introduced as impurities of the NO gas supply (Air Liquide Monoxyde d' Azote N20) and the balance gas was He. The operation temperature was controlled by means of a PID controller and a thermocouple mounted on the outer surface of the tubular reactor in the range 30–400 °C.

A second thermocouple, the tip of which touched the center of the bed was used to measure the temperature inside the catalytic reactor. The experiments were carried out both under steady state and gradient temperature conditions. Before each measurement the catalyst was regenerated under helium flow (35 ml min^{-1}) at a temperature of 250 °C. During the steady state temperature experiments, kinetic data were taken, every 30 min after a period of at least 5 min on the reactants stream. The concentrations of NO, N_2O, CO_2, CO, N_2 and O_2 were analyzed alternatively at the inlet and outlet of the reactor with a gas chromatograph GC (SRI 8610C), equipped with a six port gas-sampling valve and TCD detector. A Heysep D packed column (1/8 in. SS) of 10 m length ensured satisfactory resolution of NO, N_2, O_2 and CO at a GC furnace temperature of 30 °C CO_2 was eluted 10 min after injection in a temperature of 100 °C. Thus the cool-down capacity of the GC furnace determined the frequency of gas sampling. The system was calibrated with concentrations of 1, 3, 5, 10, and 15% (v/v) for all the examined gases.

3. Results and discussion

3.1. Material characterisation

In order to obtain porous carbon metal composites, crosslinking of the polymeric precursors prior to pyrolysis was necessary to ensure the formation of an interconnected polymer network (uncrosslinked precursors led to final products with collapsed, non porous structures). It has already been established that alginate can form stable structures in the presence of divalent metals such as copper ions. However, when copper ions are used as the crosslinking agent, there is limited control over the metal content of the final carbon, since stable structures can be achieved only when copper ions concentration in the crosslinking solution exceeds 500 mg L^{-1}.

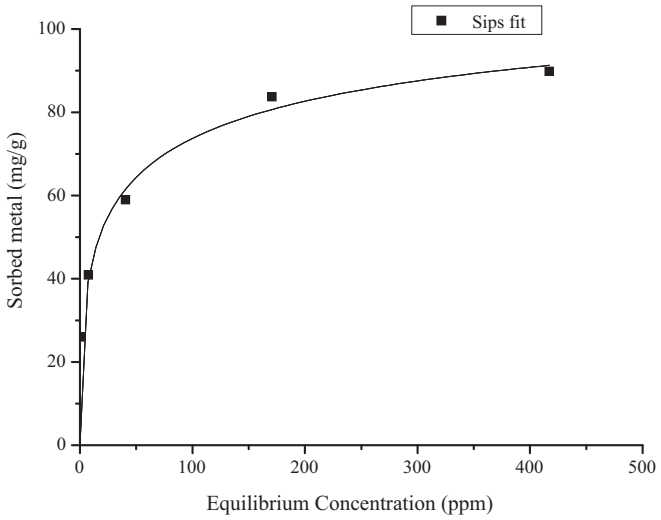

Fig. 1. Copper sorption isotherm of the precursor and Sips fitting.

In order to overcome this metal content minimum limit a crosslinking solution based on a dialdehyde was used for the preparation of the particles. Alginate alcohol groups react with aldehydes in acid media to form water insoluble polyacetals [28]. Reaction with dialdehydes is expected to form an acetal cross-linked structure as indicated by the following scheme (acetalization):

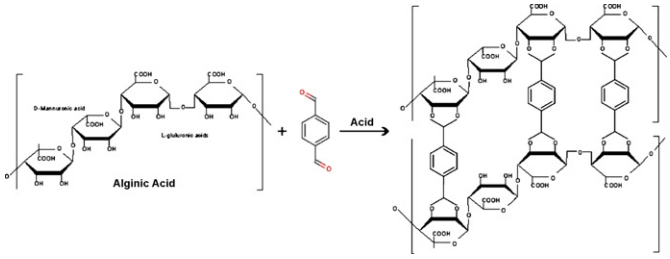

In this work, terephthalaldehyde was chosen as the crosslinking dialdehyde as it contains an aromatic ring, which results in increased carbon yield and higher specific surface areas/porosities after carbonisation.

Since the amount of metal sorbed remains in the form of metal nanoparticles after the carbonisation procedure and the mass lost during carbonisation is due to organic matter decomposition one can predefine the final product metal content by controlling the concentration of the initial metal solutions. In any case, the maximum metal content will be limited by the q_m value determined by the precursors metal sorption isotherm.

In order to investigate the relationship between the initial copper doping concentration and final carbon metal content (which depends on the metal sorbing properties of the precursor), the copper sorption isotherm of the alginate–terephthalaldehyde beads was experimentally determined at 25 °C. As seen in Fig. 1, the copper sorption isotherm follows the Sips equation with a maximum sorption significantly higher (q_m = 127.25 mg g^{-1}) than the calcium crosslinked beads investigated in a previous work (q_m = 89.56 mg g^{-1}) [27].

In this study the material loses almost 70% of its mass during carbonisation as determined by thermogravimetric analysis. By combining the metal sorption isotherm and TGA results (TGA data not presented in this study) the existence of a direct relationship between precursor metal loading and carbon metal content was revealed. Hence copper content of the final product can be preselected between 3 and 30% (w/w) by adjusting the initial metal concentration during alginate metal sorption (Table 1).

Table 1
Weight loss during carbonisation and copper content of the produced carbon/copper composites.

Nominal Cu^{2+} concentration (ppm)	Carbonisation weight loss (%)	Copper content (%)
10	70.74	3.07
50	71.04	14.13
100	72.16	21.20
250	68.46	27.66
500	68.54	30.26

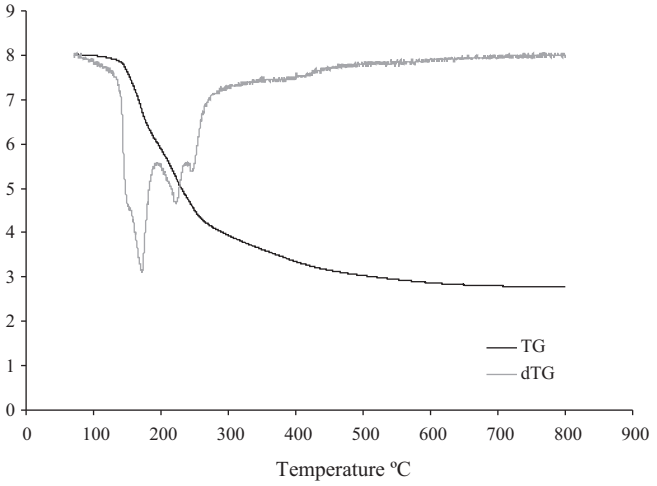

Fig. 2. TGA plot of the carbonisation process of the alginate metal containing precursor.

The possible mechanism of the metal ions reduction from ethylene glycol has been described by Eriksson et al. [29]. Specifically, two intermediate phases form during the reaction. The first phase is believed to consist of layers of metal hydroxides with intercalated molecules of ethylene glycol and is present during the heating. The second phase, occurring at 195 °C is ethylene glycolate sharing an oxygen atom with the metal hydroxide. In the case of alginate, the process followed can be considered as a modified polyol process. The metal ions bound to the carboxyl groups are in the close vicinity of the hydroxyl groups of the uronic acid residues that act as the intercalated ethylene glycol molecules in the first step of the polyol process [30].

As seen from the dTG data in the TGA graph (Fig. 2) the mass loss representing the second phase of the polyol process is observed at ≈175 °C somewhat lower than the one reported by Eriksson et al. probably due to the tighter structure of the alginate-metal matrix compared to the intercalated ethylene glycol–metal system.

The N_2 adsorption isotherm at −196 °C (Fig. 3) of the C/Cu nanoparticles composite is type I isotherm, indicating the presence of large fractions of micropores, while the isotherm of uncrosslinked sample can be considered as non-porous. Specific surface areas were calculated according to the BET method. Total pore volumes were directly derived from the adsorbed quantity at high relative pressures ($p/p_0 \sim 0.95$). Thus for the sample with 20% (w/w) Cu a specific surface area of 450–500 m^2 g^{-1}, and a total pore volume of 0.22 ml g^{-1} were determined. Adsorption data were analyzed by NLDFT equilibrium model for slit pores and the pore size distributions (PSD) were calculated [31]. It can be seen that the majority of pore volume lies below 0.75 nm.

In addition, a very interesting feature of the nitrogen adsorption isotherms is the low-pressure hysteresis. This could be attributed to kinetic reasons, i.e., the possible existence of constrictions, which hinder the access to certain pores [32].

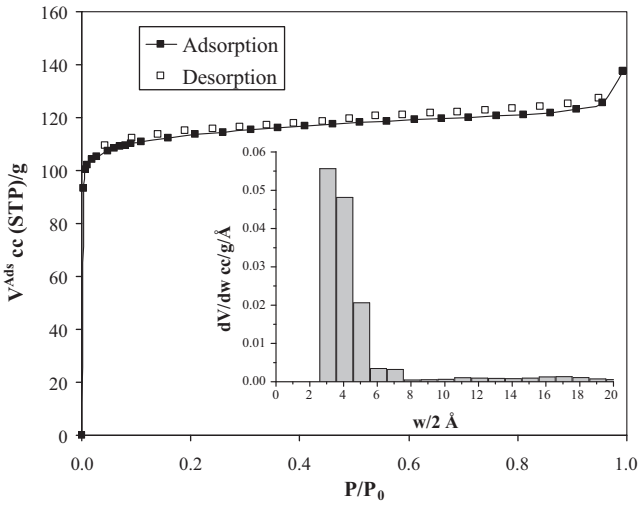

Fig. 3. Nitrogen adsorption isotherm at −196 °C, insert: pore size distribution using NLDFT.

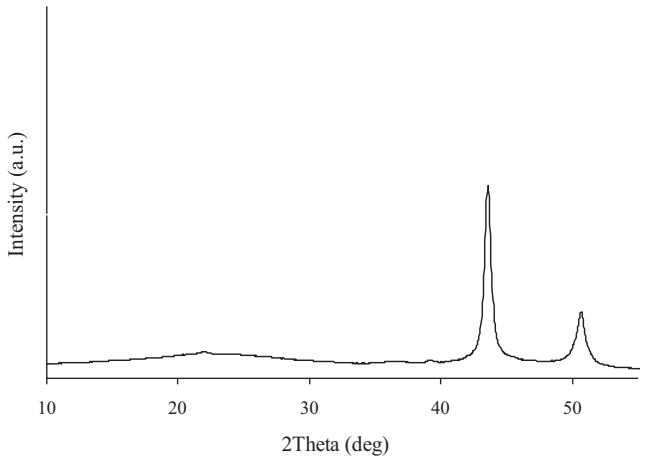

Fig. 4. XRD pattern of the carbon/Cu nanocomposite material.

In the XRD spectra (Fig. 4) the main peaks around 43° and 51° are due to Cu° (1 1 1 and 2 0 0, respectively) while the absence of the small characteristic peaks around 40°, due to CuO, indicates the quantitative reduction of copper ions to metallic copper. From the width of the peak around 43° the mean size of the metal nanoparticles was determined, using the Scherrer formula:

$$t = \frac{K\lambda}{B\cos\theta_B}$$

where t is the averaged dimension of crystallites; K is the Scherrer constant, somewhat arbitrary value that falls in the range 0.87–1.0 (it is usually assumed to be 0.89); λ is the wavelength of X-ray; B is the integral breadth of a reflection (in radians 2θ) located at 2θ.

The mean particle size was found to be independent of metal loading and around 10–15 nm.

SEM images of the C/Cu nanoparticles samples (Fig. 5) showed that for all samples, the nanoparticles are of a fairly spherical shape while the corresponding EDX spectrum identified the presence of copper. Since the metal particles are formed at the metal binding sites of the precursor, it is obvious that they are very well dispersed into the whole mass of the carbon material. The copper nanoparticles are mainly sited on the external pore walls, leaving the porosity almost unaffected by the metal content. The average copper particle size is in agreement with the results obtained from XRD analysis.

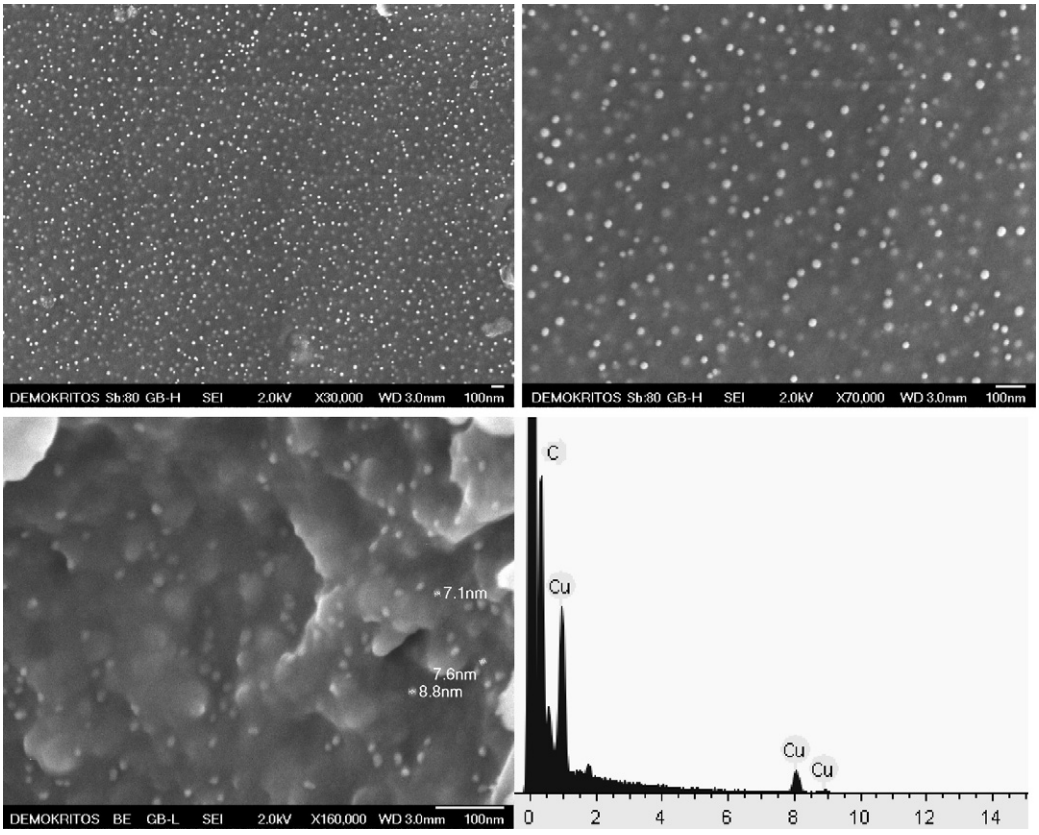

Fig. 5. SEM images and EDX spectrum of the produced carbon/copper composites surface (doping with 100 mg L^{-1} Cu^{2+}, 30% (w/w) Cu in the final product).

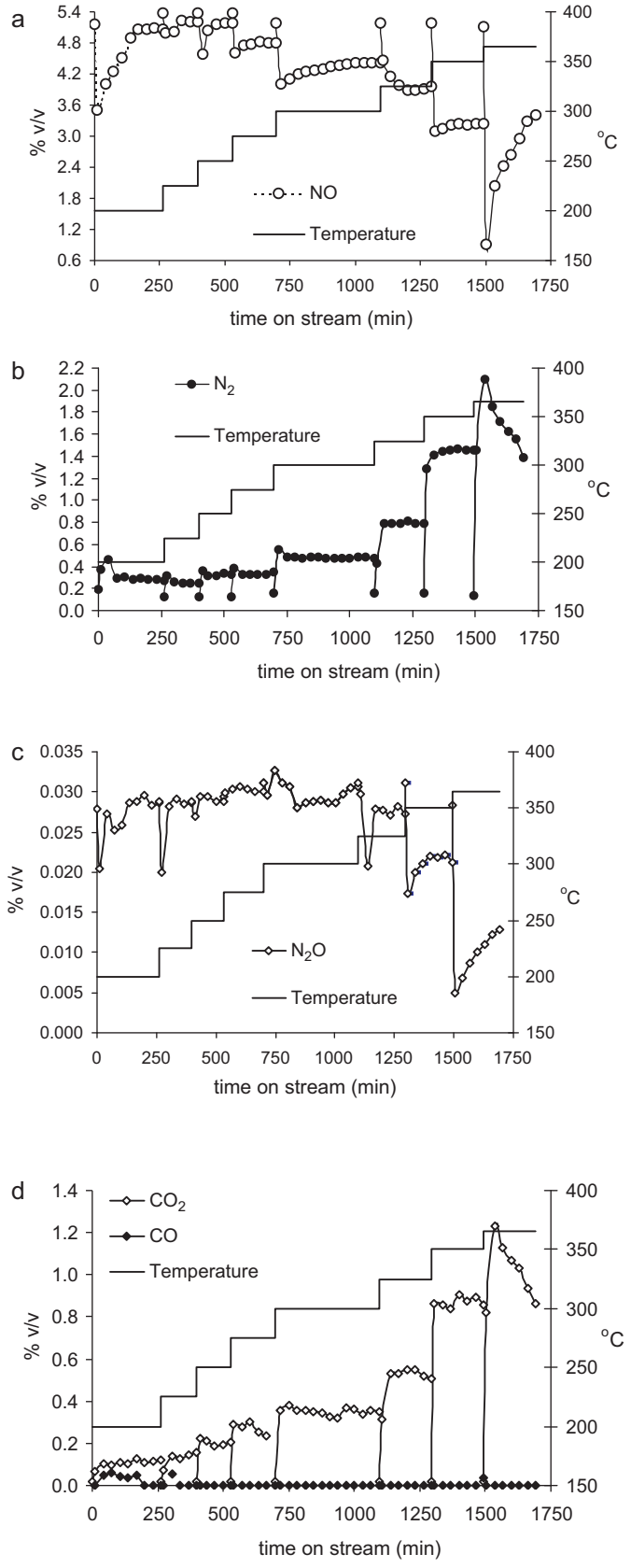

Fig. 6. Catalytic NO_x conversion: (a) NO, (b) N_2, (c) N_2O, (d) CO and CO_2 effluent concentration vs. time on stream.

3.2. Evaluation of catalytic properties

The resulting C/Cu nanoparticles composites of tunable metal content prepared by this facile and quick method, exhibit excellent dispersion of spherical nanoparticles even up to 30% (w/w) Cu. Such materials are excellent candidates for their applications as catalysts in NO reduction. To this end experiments were conducted for the evaluation of the catalytic properties, of a relatively high loaded material (20%, w/w Cu).

The evolution with time of the gases concentration in the effluent stream of the reactor as a function of temperature is presented in Fig. 6. The first data point at each temperature corresponds to a bypass measurement showing the composition of each gas in the feed.

It can be seen (Fig. 6a) that the developed catalyst is active even at a temperature of 200 °C which is among the lowest ever reported for carbon supported metal catalysts evaluated in NO_x abatement applications [33–37]. This can be considered a result of the copper nanoparticles very small size, their good distribution over the carbon support (Fig. 5) and indicates that due to the catalyst development technique particle agglomeration was avoided.

Interestingly, at 200 °C, the steady state conversion of NO was achieved after almost 2 h on stream whereas during the subsequent temperature increments up to 275 °C, the transient state period was less than 1 h. This fact indicates that the mechanism behind the NO abatement is the copper catalyzed scission of NO and that the key factor for an improved steady state conversion is the stoichiometric oxidation of the carbon support by the adsorbed oxygen. Specifically, at the initial stages of the catalytic test (low temperatures) the oxygen produced by the NO scission is continuously adsorbed on the catalyst leading to a gradual saturation of the active metal sites. From then on each temperature increase results in the partial desorption of a portion of the adsorbed oxygen species and the enhancement of the NO dissociation rate. Both these phenomena contribute to the faster catalyst saturation (e.g. lower amount of free active metal sites in combination with higher *–O production rate). From 300 °C and up to 350 °C the significant contribution of the carbon support can be noticed as it acts as a reducing agent and removes efficiently the produced *–O species in the form of CO_2.

Illan-Gomez et al. [10,16] reported that during NO–carbon reaction, metal species participate in a redox mechanism, where the metal is oxidized by NO and reduced by carbon. As a consequence, the catalyst behaviour is related to the initial state of metal before reaction (preferentially in a reduced state), its affinity towards NO and its redox properties. In fact, carbon can be used both as a reducing agent and as a catalyst support. Metals are able to dissociatively chemisorb NO [16], but this compound can also be chemisorbed on the surface of the active carbon [38] and, as a result, surface oxides appear, while N_2 is released [39].

As seen in Table 2 the catalytic activity of the prepared material is significantly higher than other elaborately prepared materials such as Rh nanoparticles supported on single wall CNT's and remains almost stable throughout the experimental time on stream at each examined temperature. The catalytic abatement of NO resulted to a product distribution which presented an almost 100% selectivity for N_2 during the steady state stage. The N_2O concentration remains unchanged up to 325 °C showing that the *–N species are preferably desorbed as N_2(g) rather than as N_2O(g) in combination with the *–NO species. Moreover a considerable degree of N_2O reduction to N_2 can be observed for the temperatures of 325 and 350 °C.

Finally, signs of the carbon support deterioration were observed at 365 °C. This can be attributed to the high NO concentrations used in this study in order to evaluate the material under severe

Table 2
Catalytic conversion data and comparison.

Temperature (°C)	Steady state conversion (%)	Initial conversion (%)	Steady state conversion Rh/SWCNT's (%) [33]
450	N/A	N/A	99
400	N/A	N/A	52
365	37.3	83	
350	37.7	40	9
325	24.4	24	
300	14.8	22	3
275	10.3	14	
250	3.7	14	2
225	2.8	6.8	
200	1.9	5.3	

pollutant loading, being up to 50 times higher than the ones usually reported in the recent literature [33]. Under these conditions a high amount of oxygen is produced during NO dissociation that would be avoided under NO concentrations similar with those often applied in other studies. Despite these extreme NO loadings the material exhibited very good NO reduction efficiency and it is expected that catalyst with higher metal content (up to ~30%, w/w) will exhibit enhanced catalytic NO reduction properties. Further experiments will concentrate on the study of the catalytic properties of the material under realistic lean and rich exhaust gas compositions (including O_2, CO_2, and CO hydrocarbon traces).

4. Conclusions

A chemical crosslinking procedure was employed for the preparation of an alginate based sorbent with exceptional metal retention properties that was used as a precursor for the preparation of a carbon/copper nanoparticles composite material by a facile one step carbonisation–reduction procedure.

The prepared material shows a very good dispersion of copper nanoparticles of fairly uniform size. Metal loading can be preselected between 3 and 30% (w/w) Cu by adjusting the initial copper doping of the precursor.

Even at high metal loading no visible aggregations of metal particles are evident due to the dispersion of the active metal binding sites in the precursor.

The material shows very promising catalytic activity in NO reduction applications, which starts already at temperatures among the lowest ever reported for carbon supported metal catalysts evaluated in NO reduction applications. Due to the high metal loading and the lack of nanoparticles aggregation the steady state activity was satisfactory at high NO concentrations up to 50 times higher than recent literature data.

Acknowledgements

This study was partially supported by the European Network of Excellence (NoE) Inside Pores (NMP3-CT2004-500895).

The authors would like to thank Dr. G.Ch. Charalampopoulou for her very constructive suggestions.

References

[1] Y. Li, X. Duan, Y. Qian, L. Yang, H. Liao, Nanocrystalline silver particles: synthesis, agglomeration, and sputtering induced by electron beam, J. Colloid Interface Sci. 209 (1999) 347–349.
[2] P.V. Kamat, Photophysical, photochemical and photocatalytic aspects of metal nanoparticles, J. Phys. Chem. B 106 (2002) 7729–7744.
[3] F. Bonet, S. Grugeon, R. Herrera Urbina, K. Tekaia-Elhsissen, J.-M. Tarascon, In situ deposition of silver and palladium nanoparticles prepared by the polyol process, and their performance as catalytic converters of automobile exhaust gases, Solid State Sci. 4 (2002) 665–670.
[4] S. Mann, G.A. Ozin, Synthesis of inorganic materials with complex form, Nature 382 (1996) 313–318.
[5] S.-J. Park, B.-J. Kim, Y.-S. Lee, M.-J. Cho, Influence of copper electroplating on high pressure hydrogen-storage behaviors of activated carbon fibers, Int. J. Hydrogen Energy 33 (2008) 1706–1710.
[6] M.C. Daniel, D. Astruc, Gold nanoparticles: assembly, supramolecular chemistry, quantum-size-related properties, and applications toward biology, catalysis, and nanotechnology, Chem. Rev. 104 (2004) 293–316.
[7] R.A. Catalão, F.J. Maldonado-Hódar, A. Fernandes, C. Henriques, M.F. Ribeiro, Reduction of NO with metal-doped carbon aerogels, Appl. Catal. B 88 (2009) 135–140.
[8] H. Yamashita, H. Yamada, A. Tomita, Reaction of nitric oxide with metal-loaded carbon in the presence of oxygen, Appl. Catal. 78 (1991) L1–L6.
[9] A. Tomita, Suppression of nitrogen oxides emission by carbonaceous reductants, Fuel Process. Technol. 71 (2001) 53–70.
[10] M.J. Illán-Gómez, A. Linares-Solano, L.R. Radovic, C. Salinas-Martinez, de. Lecea, NO reduction by activated carbons. 7. Some mechanistic aspects of uncatalyzed and catalyzed reaction, Energy Fuels 10 (1996) 158–168.
[11] M.J. Lázaro, I. Suelves, R. Moliner, S.V. Vassilev, C. Braekman-Danheux, Low cost catalytic sorbents for NOx reduction. 2. Tests with no reduction reactives, Fuel 82 (2003) 771–782.
[12] J. Yang, G. Mestl, D. Herein, R. Schlögl, J. Find, Reaction of NO with carbonaceous materials: 1. Reaction and adsorption of NO on ashless carbon black, Carbon 38 (2000) 715–727.
[13] M.J. Illan-Gomez, A. Linares-Solano, C. Salinas-Martınez de Lecea, J.M. Calo, Nitrogen oxide (NO) reduction by activated carbons. 1. The role of carbon porosity and surface area, Energy Fuels 7 (1993) 146–154.
[14] B.R. Stanmore, V. Tschamber, J.F. Brilhac, Oxidation of carbon by NOx, with particular reference to NO_2 and N_2O, Fuel 87 (2008) 131–146.
[15] Z Schay, H. Knozinger, L. Guczi, G. Pal-Borbely, On the mechanism of NO decomposition on Cu-ZSM-5 catalysts, Appl. Catal. B 18 (1998) 263–271.
[16] M.J. Illan-Gomez, E. Raymundo-Pinero, A. Garcıa-Garcıa, A. Linares-Solano, C. Salinas-Martınez de Lecea, Catalytic NOx reduction by carbon supporting metals, Appl. Catal. B 20 (1999) 267–275.
[17] Y. Zhang, C. Erkey, Preparation of supported metallic nanoparticles using supercritical fluids: a review, J. Supercrit. Fluids 38 (2006) 252–267.
[18] P. Claus, A. Brückner, C. Mohr, H. Hofmeister, Supported gold nanoparticles from quantum dot to mesoscopic size scale: effect of electronic and structural properties on catalytic hydrogenation of conjugated functional groups, J. Am. Chem. Soc. 122 (2000) 11430–11439.
[19] K. Okitsu, S. Nagaoka, S. Tanabe, H. Matsumoto, Y. Mizukoshi, Y. Nagata, Sonochemical preparation of size-controlled palladium nanoparticles on alumina surface, Chem. Lett. 3 (1999) 271–272.
[20] J.M. Miller, B. Dunn, T.D. Tran, R.W. Pekala, Deposition of ruthenium nanoparticles on carbon aerogels for high energy density supercapacitor electrodes, J. Electrochem. Soc. 144 (1997) L309–311.
[21] E. Bekyarova, K. Kaneko, Structure and physical properties of tailor-made Ce, Zr-doped carbon aerogels, Adv. Mater. 12 (2000) 1625–1628.
[22] T.F. Baumann, G.A. Fox, J.H. Satcher, N. Yoshizawa, R. Fu, M.S. Dresselhaus, Synthesis and characterization of copper-doped carbon aerogels, Langmuir 18 (2002) 7073–7076.
[23] F. Bonet, V. Delmas, S. Grugeon, R. Herrera Urbina, P.-Y. Silvert, K. Tekaia-Elhsissen, Synthesis of monodisperse Au, Pt, Pd, Ru and Ir nanoparticles in ethyleneglycol, Nanostruct. Mater. 11 (1999) –1284.
[24] C.-Y. Lu, M.-Y. Wey, Y.-H. Fu, The size, shape, and dispersion of active sites on AC-supported copper nanocatalysts with polyol process: the effect of precursors, Appl. Catal. A 344 (2008) 36–44.
[25] E.C. Vermisoglou, A. Labropoulos, G.E. Romanos, E. Kouvelos, S. Papageorgiou, G.N. Karanikolos, F. Katsaros, N.K. Kanellopoulos, J. Nanosci. Nanotechnol. 10 (2010) 1–10.
[26] P. Chen, X. Zhang, Z. Miao, B. Han, G. An, Z. Liu, In-situ synthesis of noble metal nanoparticles in alginate solution and their application in catalysis, J. Nanosci. Nanotechnol. 9 (2009) 2628–2633.
[27] S.K. Papageorgiou, F.K. Katsaros, E.P. Kouvelos, J.W. Nolan, H. Le Deit, N.K. Kanellopoulos, Heavy metal sorption by calcium alginate beads from *Laminaria digitata*, J. Hazard. Mater. 137 (2006) 1765–1772.
[28] W.R. Sorenson, T.W. Campbell, Preparative Methods in Polymer Chemistry, Interscience Publisher, 1961, p. 176.
[29] G. Eriksson, H. Siegbahn, S. Andersson, T. Turkki, M. Muhammed, The reduction of Co^{2+} by polyalcohols in the presence of WC surfaces studied by XPS, Mater. Res. Bull. 32 (1997) 491–499.
[30] Y. Fang, S. Al-Assaf, G.O. Phillips, K. Nishinari, T. Funami, P.A. Williams, L. Li, Multiple steps and critical behaviors of the binding of calcium to alginate, J. Phys. Chem. B 111 (2007) 2456–2462.
[31] P.I. Ravikovitch, A. Vishnyakov, R. Russo, A.V. Neimark, Unified approach to pore size characterization of microporous carbonaceous materials from N2, Ar, and [2CO] adsorption isotherms, Langmuir 16 (2000) 2311–2320.
[32] F.K. Katsaros, Th.A. Steriotis, G.E. Romanos, M. Konstantakou, A.K. Stubos, N.K. Kanellopoulos, Preparation and characterisation of gas selective microporous carbon membranes, Micropor. Mesopor. Mater. 99 (2007) 181–189.
[33] H. Beyer, K. Kohler, NOx removal by rhodium catalysts supported on carbon nanotubes: evidence for the stoichiometric reduction of NO_2 and NO by the carbon support, Appl. Catal. B 96 (2010) 110–116.
[34] S.J. Wang, W.X. Zhu, D.W. Liao, C.F. Ng, C.T. Au, In situ FTIR studies of NO reduction over carbon nanotubes (CNTs) and 1 wt.% Pd/CNTs, Catal. Today 95 (2004) 711–714.

[35] S.H. Tang, B.C. Liu, Q. Liang, L.Z. Gao, L.F. Zhang, Z.L. Yu, NO decomposition on Rh supported CNTs, Chin. Chem. Lett. 12 (2001) 83–86.
[36] J.Z. Luo, L.Z. Gao, Y.L. Leung, C.T. Au, The decomposition of NO on CNTs and 1 wt% Rh/CNTs, Catal. Lett. 66 (2000) 91–97.
[37] H. Beyer, K. Chatziapostolou, K. Kohler, Abatement of NO using rhodium catalysts supported on carbon nanotubes: carbon as support material and reducing, Agent Top. Catal. 52 (2009) 1752–1756.
[38] C. Pevida, A. Arenillas, F. Rubiera, J.J. Pis, Heterogeneous reduction of nitric oxide on synthetic coal chars, Fuel 84 (2005) 2275–2279.
[39] E.M. Suuberg, H. Teng, Chemisorption of nitric oxide on char. 1. Reversible nitric oxide sorption, J. Phys. Chem. 97 (1993) 478–483.